Delayed-onset ataxia in mice lacking α-tocopherol transfer protein: Model for neuronal degeneration caused by chronic oxidative stress

Takanori Yokota*†, Keiji Igarashi‡, Toshiki Uchihara§, Kou-ichi Jishage¶, Hiroshi Tomita‖, Akira Inaba*, Yi Li*, Makoto Arita‡, Hiroshi Suzuki¶, Hidehiro Mizusawa*, and Hiroyuki Arai†‡

*Department of Neurology, Tokyo Medical and Dental University, 1-5-45 Yushima, Bunkyo-ku, Tokyo 113-8519, Japan; ‡Department of Health Chemistry, University of Tokyo, 7-3-1 Hongo, Bunyo-ku, Tokyo 113-0013, Japan; §Department of Neuropathology, Tokyo Metropolitan Institute for Neuroscience, 2-6 Musashidai, Fuchu-shi, Tokyo 183-8526, Japan; ¶Pharmaceutical Technology Laboratory, Chugai Pharmaceutical Company, Ltd., 1-135 Komakado, Gotenba, Shizuoka 412-8513, Japan; and ‖Department of Ophthalmology, Tohoku University, 1-1 Seiryo-cho, Aoba-ku, Miyagi 980-8574, Japan

Edited by E. R. Stadtman, National Institutes of Health, Bethesda, MD, and approved October 25, 2001 (received for review August 29, 2001)

α-Tocopherol transfer protein (α-TTP) maintains the concentration of serum α-tocopherol (vitamin E), one of the most potent fat-soluble antioxidants, by facilitating α-tocopherol export from the liver. Mutations of the α-TTP gene are linked to ataxia with isolated vitamin E deficiency (AVED). We produced a model mouse of AVED by deleting the α-TTP gene, which showed ataxia and retinal degeneration after 1 year of age. Because the brain α-TTP functions in maintaining α-tocopherol levels in the brain, α-tocopherol was completely depleted in the α-TTP$^{-/-}$ mouse brain, and the neurological phenotype of α-TTP$^{-/-}$ mice is much more severe than that of wild-type mice when maintained on an α-tocopherol-deficient diet. Lipid peroxidation in α-TTP$^{-/-}$ mice brains showed a significant increase, especially in degenerating neurons. α-Tocopherol supplementation suppressed lipid peroxidation and almost completely prevented the development of neurological symptoms. This therapy almost completely corrects the abnormalities in a mouse model of human neurodegenerative disease. Moreover, α-TTP$^{-/-}$ mice may prove to be excellent animal models of delayed onset, slowly progressive neuronal degeneration caused by chronic oxidative stress.

Ataxia with isolated vitamin E deficiency (AVED) is an autosomal recessive disease, the phenotype of which is often indistinguishable from Friedreich ataxia (1), the most common hereditary ataxia in Europe and United States. We cloned the α-tocopherol transfer protein (α-TTP) gene (2) and identified mutations on the α-TTP gene in patients with AVED (3, 4). Later, we found those same mutations on the α-TTP gene to be a cause of retinitis pigmentosa as well (5, 6). α-TTP is expressed in the brain and retina as well as in the liver, and its function still remains unclear (6, 7). Therefore, it is not known whether α-tocopherol deficiency is the only cause for neuronal degeneration of AVED. Here we produced a model mouse of AVED by deleting the α-TTP gene. The mice showed ataxia and retinal degeneration after 1 year of age, and these symptoms were reversed after α-tocopherol supplementation.

The brain is thought to be particularly vulnerable to oxidative stress (8), and accumulating evidence suggests that oxidative stress is involved in the pathogenesis of neurodegenerative diseases including Alzheimer's disease and amyotrophic lateral sclerosis (8, 9). In animal models, neuronal cell death has been induced by free radical-producing chemicals, such as paraquat (10) or *N*-methy-4-phenyl-1,2,3,6-tetrahydropyridine (MPTP; ref. 11), or by knocking out the manganese superoxide dismutase gene (12). These experimentally induced neuronal degenerations develop acutely within several days and differ therefore from the cell death that occurs in human neurodegenerative diseases, which are characterized by delayed onset and slow progression over years or decades. We discuss whether the α-TTP$^{-/-}$ mouse serves as a mouse model of age-related neuronal degeneration arising from chronic oxidative stress.

Materials and Methods

Generation of α-TTP Knockout Mice. Details are reported elsewhere (13). In brief, an α-TTP-targeting vector was constructed from an 8.8-kb α-TTP genome fragment including exon 1. We inserted a fragment of phosphoglycerate kinase-neo cassette into exon 1 and flanked an herpes simplex virus thymidine kinase gene downstream of exon 2. The construct was electroporated into AB2.2-Prime embryonic stem cells. G418/gancyclovir-resistant clones were screened by PCR, and then embryonic stem cells containing the disrupted allele were injected into C57BL/6J blastocysts. The resulting male chimeras were bred with C57BL/6 females. α-TTP$^{-/-}$ mutant mice were produced from α-TTP$^{+/-}$ crosses. The mice studied were of a mixed (50% C57BL/6J and 50% 129/SvEvBrd) genetic background.

Wild-type and α-TTP$^{-/-}$ mice were fed on a normal (36 mg of α-tocopherol/kg), α-tocopherol-supplemented (600 mg of α-tocopherol/kg), or α-tocopherol-deficient diet. These diets were prepared from a vitamin E-deficient diet (Funabashi Farm, Chiba, Japan) containing 20% vitamin free-casein/25% glucose/25% sucrose/15% α-cornstarch/5% cellulose powder/mixed vitamins except α-tocopherol supplemented with 10% (wt/wt) stripped corn oil (Tama Biochemical, Tokyo, Japan) and D-α-tocopherol. These diets were started at weaning and continued until the animals were killed. Experiments were performed with 4–12 mice per group consisting of 50% male and 50% female.

Motor Performance Tests/Accelerating Rotating Rod Test. The mice were tested at 18 months of age. The rotating rod apparatus (Accelerating Model, Ugo Basile Biological Research Apparatus, Varese, Italy) was used to evaluate motor function. The mice were placed on the rod (3-cm in diameter) for four trials per day for 2 consecutive days. Each trial lasted a maximum of 10 min, during which the rotating rod underwent linear acceleration from 4 to 40 rpm over the first 5 min of the trial and then remained at maximum speed for the remaining 5 min. Animals were scored for their latency to fall (in seconds) in each trial.

Electrophysiological Analysis. *Somatosensory-evoked potential (SEP).* Mice were tested at 19–20 months of age. The mice were anesthetized with an i.p. injection of chloral hydrate (0.8 mg/g). Rectal temperatures were maintained between 35 and 37°C. For

This paper was submitted directly (Track II) to the PNAS office.

Abbreviations: AVED, ataxia with isolated vitamin E deficiency; α-TTP, α-tocopherol transfer protein; SEP, somatosensory-evoked potential; ERG, electroretinogram; TBARS, thiobarbituric acid-reactive substance(s); HNE, 4-hydroxy-2-nonenal.

†To whom reprint requests may be addressed. E-mail: tak-yokota.nuro@tmd.ac.jp or harai@mol.f.u-tokyo.ac.jp.

The publication costs of this article were defrayed in part by page charge payment. This article must therefore be hereby marked "*advertisement*" in accordance with 18 U.S.C. §1734 solely to indicate this fact.

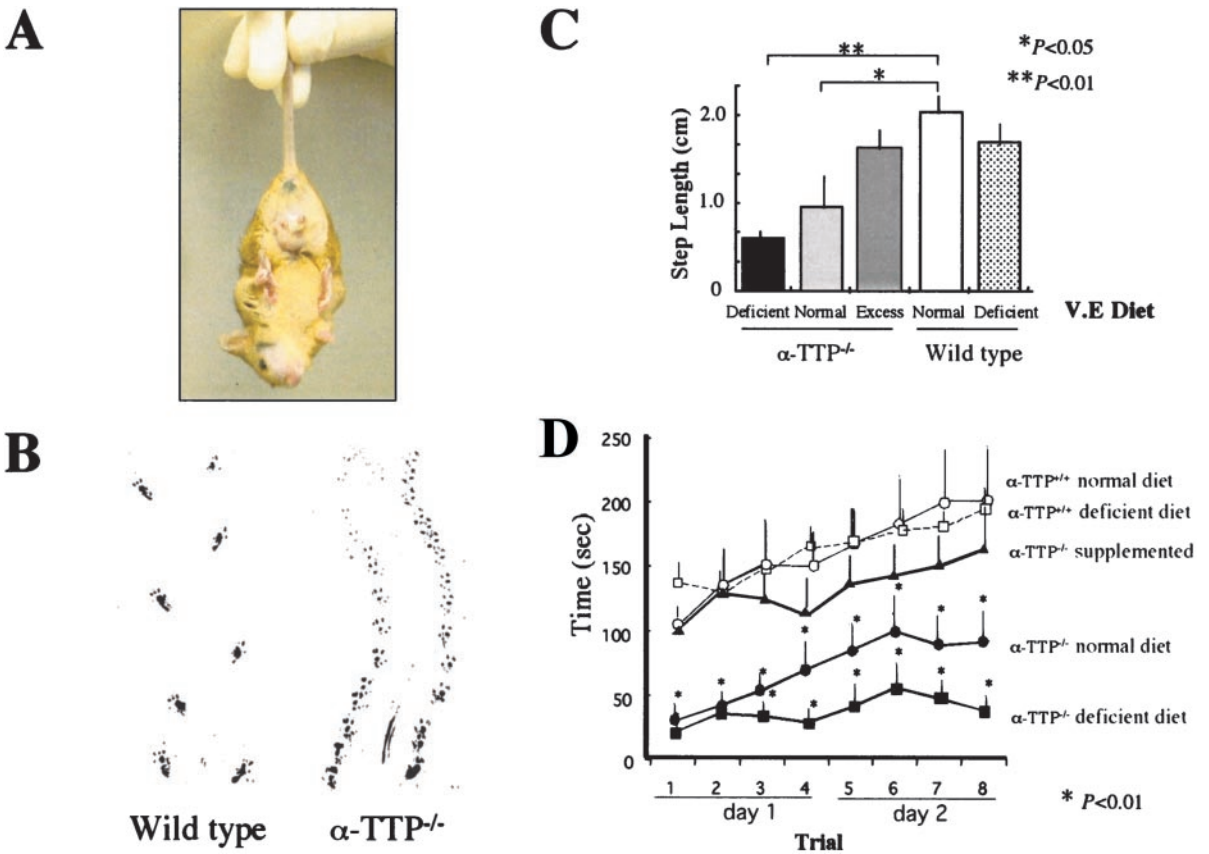

Fig. 1. Analysis of motor performance. (*A*) Dystonic posture of hind limbs of an α-TTP$^{-/-}$ mouse when the mouse was lifted by its tail. (*B*) Representative footprint patterns of a 14-month-old wild-type mouse (*Left*) and an α-TTP$^{-/-}$ mouse on an α-tocopherol-deficient diet (*Right*). (*C*) Quantitative assessment of step length. (*D*) Performances on the accelerating rotating rod apparatus; four trials per day for 2 consecutive days. α- TTP$^{-/-}$ mice had significantly shorter step length and poor performance on the rotating rod, which improved with α-tocopherol supplementation. Values are the mean and SEM. $n = 10$ for each group.

the recordings, needle electrodes were inserted s.c. over (*i*) the axilla and contralateral hand sensory area 2 mm lateral to the bregma that was referred to an electrode inserted at the base of the nose for the forelimb stimulation and (*ii*) between the fifth and sixth lumbar spinous processus that was referred to an electrode inserted 5 mm proximal to the fifth and sixth lumbar spinous processus and foot sensory area (bregma) that was referred to one inserted at the base of the nose for the hind limb stimulation. Peripheral nerves were stimulated electrically with needle electrodes inserted at the wrist or ankle at 3 Hz. The stimulus intensity was adjusted to the level at which the response from the axilla or the lumbar recording was evoked supramaximally. All recordings were made with a Neuropack 4 (Nohonkoden, Tokyo) with a bandpass 20–3,000 Hz. For the cortical potential, the first positive peak was named P1, the following negative peak was named N1, and the amplitude of P1–N1 was measured.

Electroretinogram (ERG). Mice were dark-adapted and anaesthetized with i.m. injections of xylazine (13 mg/kg) and ketamine (87 mg/kg). The corneas were anaesthetized with 0.5% propacaine hydrochloride, and the pupils were dilated with 1% atropine and 2.5% phenylephrine hydrochloride. Small contact lenses with gold wire loops were placed on both corneas and a silver wire reference electrode was placed s.c. between eyes. Stimuli with 10-μsec flashes of white light were presented at the intensities of 2.40, 0.23, and 0.0025 candelas per m^2 (-30, -10, and 0 db) at 10-s, 30-s, and 1-min intervals, respectively. Full-field scotopic ERGs were elicited, and three responses were recorded and averaged at each intensity by a UTAS-E 3000 visual electrodiagnostic system (LKC Technologies, Gaithersburg, MD) with bandpasses of 0.3–500 Hz.

Neuropathological and Immunohistochemical Analysis. Pathological analysis was done at 12 and 20 months of age. The number of mice examined was 3–6 for each group. The mice were anaesthetized with an i.p. injection of pentobarbital (60 mg/kg) and killed by transcardiac perfusion with Zanboni's solution. The brain, spinal cord, and retina were removed, postfixed in the same solution, embedded in paraffin, sectioned (8 μm), and then stained with hematoxylin/eosin, Klüver–Barrera, and Fontana–Masson. In addition, the spinal cord was postfixed also with 1% glutaraldehyde in PBS and 1% OsO_4, embedded in Epon, sectioned (1 μm), and stained with toluidine blue. Immunohistochemical analysis with antiglial fibrillary acidic protein antibody (1:1,000, Dako) was used to evaluate gliosis. Mouse eyes were fixed with 4% paraformaldehyde/0.1 M phosphate buffer, pH7.4, and sectioned with a cryostat (10 μm). Autofluorescence of lipofuscin in the retina was observed with a computerized fluorescence microscope (Leica Qfluoro 550) equipped with a filter set containing a 460–500-nm excitation filter, a dichromatic mirror at 505 nm, and a 512–542-nm emission filter. Quadriceps skeletal muscles from unfixed mice were frozen, sectioned (6 μm), and stained with hematoxylin/eosin. The seventh thoracic cord stained by the Fontana–Masson method was used for quantification of accumulated lipofuscin granules. Digitized images of the entire left anterior horn were subtracted such that each pixel represented red/green/blue values above the background level (calculated as the mean of the entire anterior horn area). They were converted to 8-bit gray-scale images that then were calibrated with two different internal references (the mean of the background was 0, and the mean of ependymal nuclei was 128; PHOTOSHOP 5). All the spots containing lipofuscin granules were picked up from the

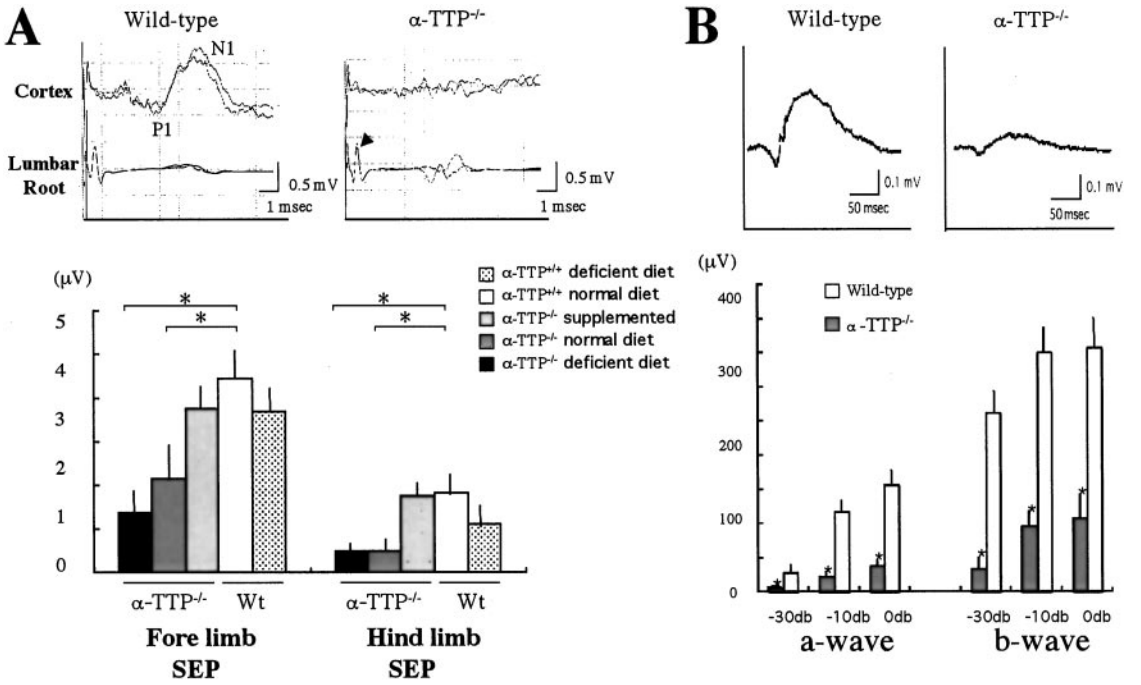

Fig. 2. Electrophysiological analysis. (*A*) SEPs: Representative wave forms from wild-type and α-TTP$^{-/-}$ mice on an α-tocopherol-deficient diet (*Upper*). Two averages of 100–300 sweeps recorded for each response are superimposed. In α-TTP$^{-/-}$ mice, the potential from the lumbar root was similar to that of wild type (arrowhead), but the cortical potential almost disappeared. Sizes of the cortical potential of SEPs were measured from N1 to P1 (*Lower*). Values are the mean and SEM. $n = 6$ for each group; *, $P < 0.01$. (*B*) ERG analysis: Representative wave forms from wild-type and α-TTP$^{-/-}$ mice on a normal diet at a stimulus intensity of -10 db (*Upper*). Sizes of the a-wave and b-wave were measured when the stimulus intensity was changed to -30, -10, and 0 db (*Lower*). Values are the mean and SEM. $n = 10$ for each group; *, $P < 0.01$.

calibrated images, and their relative intensities (0–255) and areas were measured by NIH IMAGE 1.62. The sum of the area (square μm) $\times$ the mean relative intensity (0–255) of each spot represented the relative amount of lipofuscin accumulated.

Biochemical Analysis of the Tissues and Blood. At 21 months of age, blood and tissue samples were collected from overnight-fasted mice. The heart, liver, and brain tissues were excised from mice after transcardiac perfusion with ice-cold PBS. The samples were frozen and stored at -80°C until used.

Determination of Plasma and Tissue α-Tocopherol Concentrations. The α-tocopherol concentration in the plasma was determined by the method reported previously (12). Heart and brain tissue concentrations of α-tocopherol were determined by using the method of Abe and Matsumoto (14).

Measurement of Lipid Peroxidation. *Thiobarbituric acid-reactive substances (TBARS).* The TBARS was assayed by the modified method of Tamaoka *et al.* (15). Briefly, samples were homogenized in a 50 mM Tris·HCl buffer (pH 7.6). A 100-μl sample was added to 200 μl of 8.1% (wt/vol) SDS, 1.5 ml of 20% acetic acid (pH 3.5), and 1.5 ml of 0.8% (wt/vol) thiobarbituric acid. After incubation at 95°C for 60 min, 4.0-ml samples were added to 1.0 ml of distilled water and 5.0 ml of a mixture of 1-butanol and pyridine (15:1, vol/vol). After centrifugation at 4,000 $\times$ *g* for 10 min, the absorbance of the upper layer was measured at 532 nm by using a Hitachi (Tokyo, Japan) U-1100 spectrophotometer.

Western blotting. Half of the cerebrum and cerebellum and entire spinal cord were homogenized in tissue lysis buffer. Then, 15–50 μg of each sample was boiled, separated on 12.5% SDS/PAGE minigel, and transferred to a polyvinylidene difluoride membrane. The membrane was probed with anti-α-TTP monoclonal antibody (made by K.I.) or anti-4-hydroxy-2-nonenal (HNE) monoclonal antibody (kindly given from S. Uchida), and visualized by using an ECL Western blot system (Amersham Pharmacia).

All experiments in this study were done in accordance with the Guiding Principles for the Care and Use of Research Animals of Chugai Pharmaceutical or of Tokyo Medical and Dental University.

Statistical Analysis. For multiple comparisons, single-factor ANOVA followed by the Fisher's protected least-significant difference post hoc test was used. For the analysis of ERG size, the Mann–Whitney test was used. Results were considered statistically significant at $P < 0.05$.

Results

Phenotype of α-TTP$^{-/-}$ Mice. We had described the generation and initial characterization of α-TTP$^{-/-}$ mice previously (13). The behavior of α-TTP$^{-/-}$ mice were indistinguishable from that of wild-type mice until 1 year of age, which is when α-TTP$^{-/-}$ mice on an α-tocopherol-normal and -deficient diet showed the shaking of the head and mild ataxia while walking. The onset of neurological symptoms was not markedly different between α-TTP$^{-/-}$ mice on an α-tocopherol-deficient diet and those on a normal diet. These abnormalities worsened gradually over the following months, and at the age of 18 months all α-TTP$^{-/-}$ mice had tremors and became clearly ataxic and paretic in the hind limbs while walking. Some α-TTP$^{-/-}$ mice showed dystonia (Fig. 1*A*). In α-TTP$^{-/-}$ mice, step length in footprint was shorter (Fig. 1*B*), and the performance in the rotating rod test was significantly poor in comparison to the wild-type mice (Fig. 1*D*). These disabilities were more severe in α-TTP$^{-/-}$ mice on an α-tocopherol-deficient diet, with performance improving closer to the wild-type mouse after supplementation of α-tocopherol. In contrast, the values for wild-type mice fed on the α-tocopherol-deficient diet did not differ significantly from those in wild-type mice on a normal diet (Fig. 1 *C* and *D*).

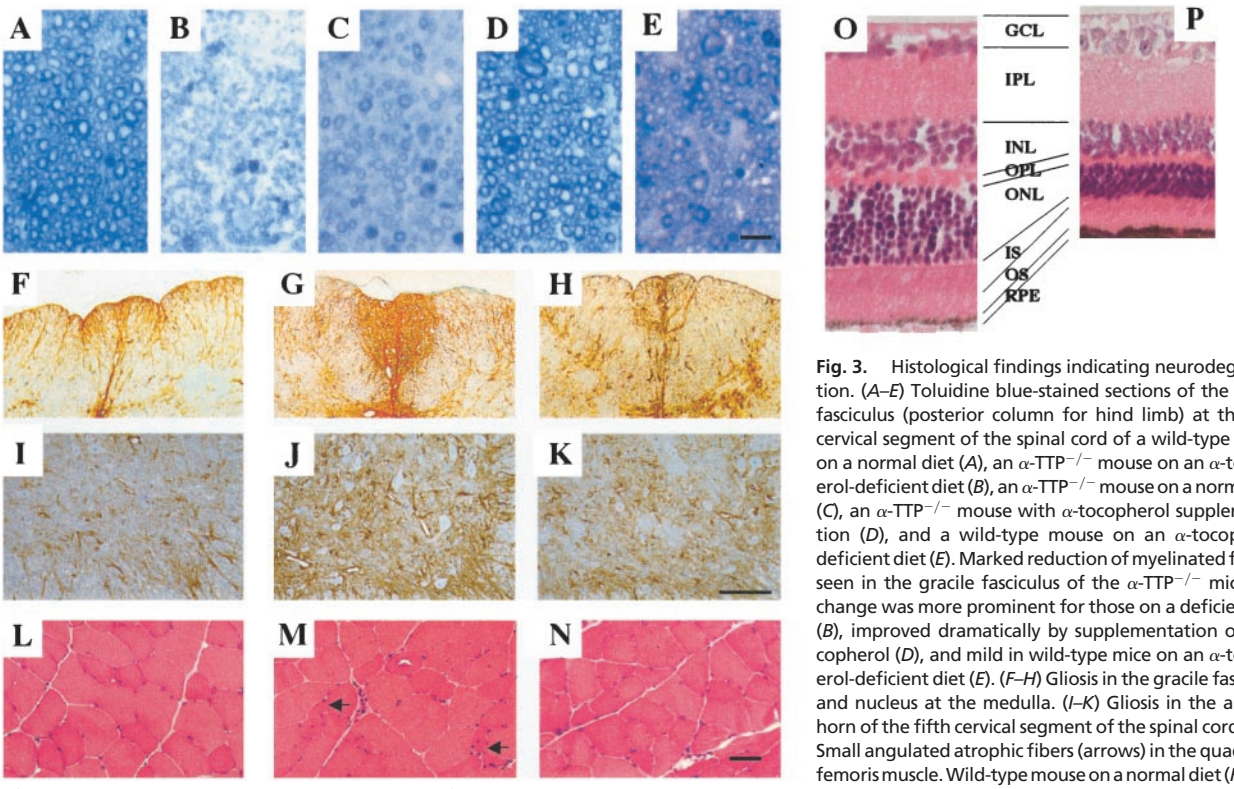

Fig. 3. Histological findings indicating neurodegeneration. (*A–E*) Toluidine blue-stained sections of the gracile fasciculus (posterior column for hind limb) at the fifth cervical segment of the spinal cord of a wild-type mouse on a normal diet (*A*), an α-TTP$^{-/-}$ mouse on an α-tocopherol-deficient diet (*B*), an α-TTP$^{-/-}$ mouse on a normal diet (*C*), an α-TTP$^{-/-}$ mouse with α-tocopherol supplementation (*D*), and a wild-type mouse on an α-tocopherol-deficient diet (*E*). Marked reduction of myelinated fibers is seen in the gracile fasciculus of the α-TTP$^{-/-}$ mice. The change was more prominent for those on a deficient diet (*B*), improved dramatically by supplementation of α-tocopherol (*D*), and mild in wild-type mice on an α-tocopherol-deficient diet (*E*). (*F–H*) Gliosis in the gracile fasciculus and nucleus at the medulla. (*I–K*) Gliosis in the anterior horn of the fifth cervical segment of the spinal cord. (*L–N*) Small angulated atrophic fibers (arrows) in the quadriceps femoris muscle. Wild-type mouse on a normal diet (*F*, *I*, and *L*), α-TTP$^{-/-}$ mouse on a normal diet (*G*, *J*, and *M*), and α-TTP$^{-/-}$ mouse with α-tocopherol supplementation (*H*, *K*, and *N*). Immunohistochemistry with anti-antiglial fibrillary acidic protein antibody (*F–K*) and stain with hematoxylin/eosin (*L–N*, *O*, and *P*). Shown also are retinal sections from wild-type mouse (*O*) and α-TTP$^{-/-}$ mouse (*P*) on a normal diet stained with hematoxylin/eosin. The thicknesses of the outer nuclear layer (ONL) and the inner (IS) and outer (OS) segments of photoreceptor cells were reduced. GCL, ganglion cell layer; IPL, inner plexiform layer; OPL, outer plexiform layer. (Scale bars: *A–E*, 25 μm; *I–K*, 100 μm; *L–N*, 50 μm.)

Electrophysiological studies were conducted by evaluating the function of the posterior column by SEP and that of the retina by ERG. In α-TTP$^{-/-}$ mice, the lumbar potentials of SEP, which arose from the spinal nerve roots, did not change (Fig. 2*A*, arrowhead), but the cortical potentials were markedly attenuated in size (Fig. 2*A*). In ERG, both the a-wave (from Müller cells and inner neuronal layers) and b-waves (from photoreceptor cells) were attenuated markedly (Fig. 2*B*).

Histological abnormalities, not obvious at the age of 12 months, became evident at 20 months of age. The major lesions in the brain of α-TTP$^{-/-}$ mice included degeneration of the posterior column and posterior column nucleus with fiber loss (Fig. 3 *B* and *C*), astrocytic proliferation (Fig. 3*G*), and numerous axonal spheroids. Anterior horn cells in the spinal cord were degenerated mildly with fibrillary gliosis (Fig. 3*J*). Skeletal muscle showed fiber size variability with small angulated atrophic fibers (Fig. 3*M*, arrows). The retina showed a disorganization of photoreceptors that consisted of reduced thickness of the outer nuclear layer and the rod inner and outer segments (Fig. 3*P*). These electrophysiological and pathological abnormalities were most obvious in α- TTP$^{-/-}$ mice on α-tocopherol-deficient diets, much milder in wild type on deficient diets, and almost disappeared in α-TTP$^{-/-}$ mice with α-tocopherol supplementation.

Biochemical Analysis of the Tissues and Blood. α-TTP protein expression in α-TTP$^{-/-}$ mice was eliminated totally in the liver on Western blots with a failure to detect even the truncated protein (data not shown). α-TTP is expressed in the wild-type brain as well as in the liver, although the expression levels in the brain are much less than those in the liver (Fig. 4*A*). To determine whether the α-tocopherol supplemented in the diet reaches the brain, we measured the tissue concentration of α-tocopherol in various brain regions of α-TTP$^{-/-}$ mice with or without supplementation of α-tocopherol. In α-TTP$^{-/-}$ mice, α-tocopherol was not detectable in the plasma and tissues (less than 0.2 μg/ml in plasma and 0.1 μg/g in tissues, data not shown in Fig. 4*B*). A dietary supplementation of α-tocopherol to α-TTP$^{-/-}$ mice increased α-tocopherol levels to 70–90% of the wild-type level in the plasma and heart (Fig. 4*B*) where α-TTP was not expressed (Fig. 4*A*). In contrast, the percentage of increase was low in the cerebrum, cerebellum, and spinal cord (6.8, 19.6, and 23.8%, respectively; Fig. 4*B*). These results indicate that α-TTP in the brain functions in maintaining the local concentration of α-tocopherol. α-Tocopherol supplementation, however, increased its content in the brain even in the absence of α-TTP, suggesting the existence of an alternative unknown pathway capable of recruiting α-tocopherol from plasma into the brain. The disappearance of neurological symptoms in α-TTP$^{-/-}$ mice by α-tocopherol supplementation indicates that a small increase in α-tocopherol in the brain (10–20% of wild-type mean value) is sufficient to prevent the development of symptoms.

Measurement of Lipid Peroxidation. The value of TBARS and specific reactivity to HNE in the α-TTP$^{-/-}$ mouse brain tissues were significantly higher than those in the wild type (Fig. 5 *A* and *B*). Massive lipofuscin accumulation was seen especially in the dorsal root ganglion cells (mother neuron of posterior column fibers; Fig. 6*B*), the outer segment of photoreceptor cells (Fig. 6*D*), and the spinal anterior horn cells (Fig. 6*G*), where neuronal degeneration occurred. Supplementation with α-tocopherol clearly suppressed all these abnormalities, indicating lipid peroxidation (Figs. 5 *A* and *B* and 6 *H* and *I*).

Discussion

The neurological symptoms and pathological findings observed in α-TTP$^{-/-}$ mice closely resemble those of AVED (1, 3, 6, 16, 17), indicating that α-TTP$^{-/-}$ mice served as a good animal models of

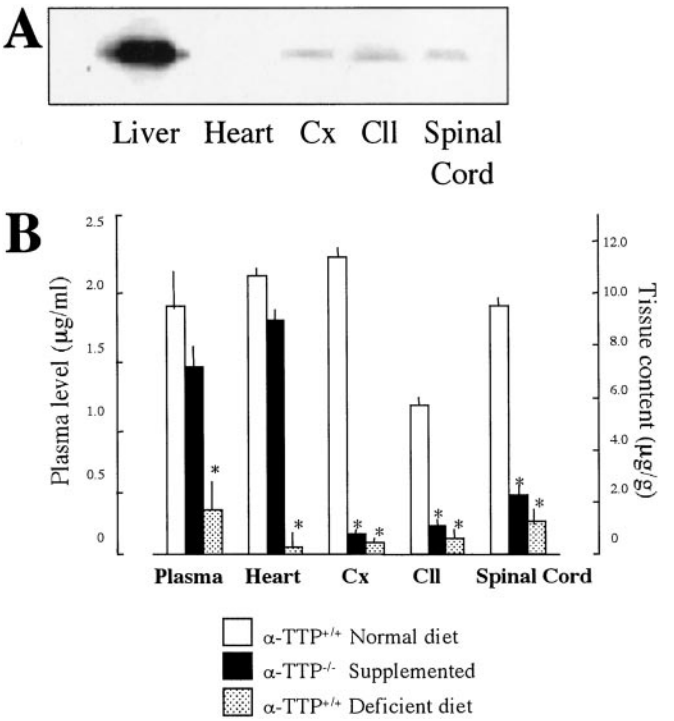

Fig. 4. α-TTP expressed in the brain maintains α-tocopherol levels in the brain, and α-tocopherol supplementation still increases its concentration in the α-TTP$^{-/-}$ mouse brain, which prevents symptoms. (*A*) Western blotting of liver, heart, cerebral cortex (Cx), cerebellum (Cll), and spinal cord from a wild-type mouse using anti-α-TTP antibody. (*B*) Plasma and tissue concentrations of α-tocopherol. In α-TTP$^{-/-}$ mice on a normal or deficient diet of α-tocopherol, α-tocopherol was depleted in plasma and each tissue (data not shown in the figure). Values are the mean and SEM. $n = 4$ for each group; *, $P < 0.001$ compared with the corresponding value of wild-type.

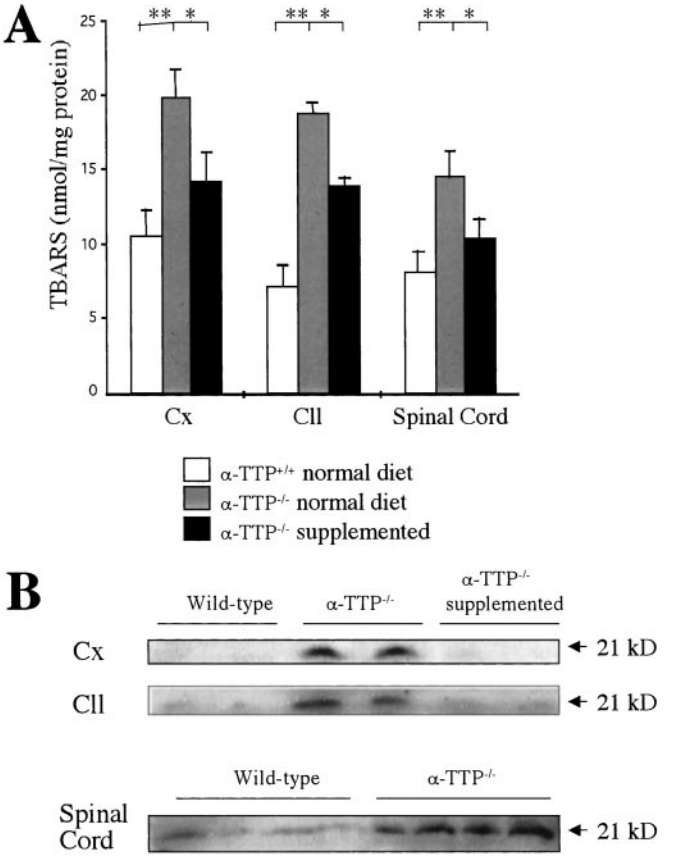

Fig. 5. Lipid peroxidation is increased in the brain of α-TTP$^{-/-}$ mice. (*A*) TBARS in the brains. Values are mean and SEM. $n = 4$ for each group; **, $P < 0.01$; *, $P < 0.01$. (*B*) Western blotting of the spinal cord from wild-type and α-TTP$^{-/-}$ mice using anti-HNE antibody. HNE-modified protein (21 kDa) is elevated significantly in α-TTP$^{-/-}$ mice as compared with wild-type or α-TTP$^{-/-}$ mice with α-tocopherol supplementation. Cx, cerebrum; Cll, Cerebellum.

AVED. The correlation between neurological phenotype and plasma and brain α-tocopherol contents was clear: α-TTP$^{-/-}$ mice with undetected plasma and brain α-tocopherols showed ataxia, whereas there was none or very mild phenotypes in α-TTP$^{-/-}$ mice fed on an α-tocopherol-excessive diet and wild-type mice with an α-tocopherol-deficient diet that had detectable plasma and brain α-tocopherols. Neurological deficits were more severe in α-TTP$^{-/-}$ mice fed on α-tocopherol-deficient diets than in α-TTP$^{-/-}$ mice fed on normal diets.

Terasawa *et al.* did not observe obvious neurological signs in their α-TTP$^{-/-}$ mice (18). The reason for this discrepancy was not clear, but small differences in genetic background or dietary factors might influence the phenotype. It was reported that 129 mice and embryonic stem cell lines derived from them had an extensive genetic variability among substrains (19). Although we used the embryonic stem cell line derived from 129/SvEvBrd strain, Terasawa's group made use of that derived from129/SvJae strain. Moreover, α-tocopherol content in the diet regimen for Terasawa's mice (≈90 mg/kg) was more than those in diets for our symptomatic mice (35 mg/kg for the normal diet and 0 mg/kg for deficient diet). Although less than 10% of the plasma α-tocopherol was detected in their TTP$^{-/-}$ mice, it was not detectable in our α-TTP$^{-/-}$ mice with normal and deficient diet, suggesting that a severe deficiency of α-tocopherol from the plasma and brain (less than 2% of wild-type mean value) is necessary to produce neurological phenotype. This is supported by a report of patients that a marked difference in neurological symptoms in siblings was observed probably caused by a small difference in plasma α-tocopherol content (0.34 vs. 0.67 μg/ml, normal, 5.7–14.3), irrespective of their having same *null* mutations of α-TTP gene (20). Our results provide a reasonable basis to treat AVED patients with α-tocopherol, and we believe that our study is the first therapy with oral administration which could almost completely prevent the development of the phenotype of animal model of human neurodegenerative disease, although there are several reports of effective therapy to delay the neurological symptoms of mouse models of human neurodegenerative diseases (21, 22).

The symptoms and pathological findings for α-TTP$^{-/-}$ mice are much more severe than those for wild type mice on α-tocopherol-deficient diet. Possible reasons for this difference are, complete elimination of α-tocopherol from the brain is not obtained by a simple dietary restriction of α-tocopherol (Fig. 4*B*), but is achieved only when the dietary restriction was combined with the deletion of the α-TTP gene. Secondly, the normal α-tocopherol concentration is much more than the minimum level for preventing neurological symptoms, as evidenced by the finding in patients with fat malabsorption that a severe, but not complete deficiency of α-tocopherol (more than 25% of the normal mean level) is not sufficient to produce neurological symptoms (23). Thirdly, the α-TTP expressed in the brain has functions other than the transfer of α-tocopherol, and the loss of these unknown functions produces neurological phenotype. This third possibility, however, is not applicable, because supplementation of α-tocopherol improved the neurological phenotype to almost normal. We therefore consider that our α-TTP$^{-/-}$ mice fed on α-tocopherol-deficient diet serve as a better model of α-tocopherol-deficient animal than wild-type mice just fed on α-tocopherol-deficient diet.

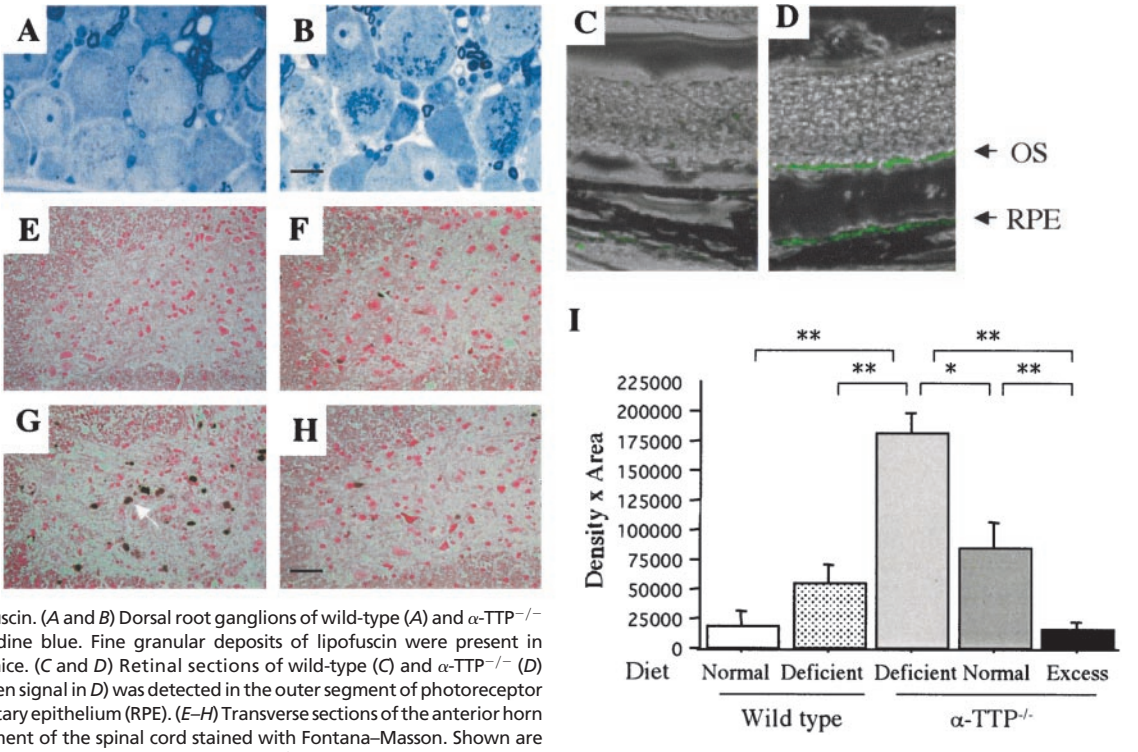

Fig. 6. Deposition of lipofuscin. (*A* and *B*) Dorsal root ganglions of wild-type (*A*) and α-TTP$^{-/-}$ mice (*B*) stained with toluidine blue. Fine granular deposits of lipofuscin were present in ganglion cells in α-TTP$^{-/-}$ mice. (*C* and *D*) Retinal sections of wild-type (*C*) and α-TTP$^{-/-}$ (*D*) mice. Autofluorescence (green signal in *D*) was detected in the outer segment of photoreceptor cells (OS) and retinal pigmentary epithelium (RPE). (*E–H*) Transverse sections of the anterior horn at the seventh thoracic segment of the spinal cord stained with Fontana–Masson. Shown are wild-type mice on normal (*E*) and deficient (*F*) diets and α-TTP$^{-/-}$ mice on a deficient diet (*G*) and supplemented with α-tocopherol (*H*). Black pigments (white arrow) show the massive accumulation of lipofuscin. (*I*) Quantitative analysis of lipofuscin in the anterior horn. The lipofuscin parameter was calculated by (area of lipofuscin, μm^2) $\times$ (relative density of lipofuscin). Values are the mean and SEM. n = 3–4 for each group; **, $P < 0.01$; *, $P < 0.01$. (Scale bars: *a–b*, 50 μm; *e–h*, 100 μm.)

We evaluated lipid peroxidation in the brain by biochemical measurement of malondialdehyde (MDA) by using the TBARS method, Western blotting with anti-HNE antibody, and quantification of lipofuscin on histology. MDA and HNE, end products of lipid peroxidation (24), are believed to be largely responsible for the cytotoxic effects observed during oxidative stress (25). Lipofuscin, yellow and autofluorescent coarse granule, is formed by reaction of protein and carbonyl compounds (26). All these products of lipid peroxidation examined were significantly increased in the α-TTP$^{-/-}$ mice and markedly improved by supplementation of α-tocopherol. Lipofuscin was accumulated especially in the neurons where neurodegeneration occurred. These indicate that the α-TTP$^{-/-}$ brain is in a highly oxidized state because of the lack of α-tocopherol, resulting in neuronal degeneration. As stated above, there are a few animal models that show rapid neuronal cell death by oxidative stress, but the α-TTP$^{-/-}$ mice are the first animal model of a late-onset, slowly progressive neuronal degeneration caused by chronic oxidative stress. Therefore, the α-TTP$^{-/-}$ mice should prove useful for investigating the mechanisms of neuronal degeneration and other age-related neurodegenerative diseases such as Alzheimer disease by crossing it with other transgenic or knockout mice of the disease.

We thank Koji Uchida, Ph.D. (Nagoya University) for providing anti-HNE antibody, Rammohan V. Rao, Ph.D. (Buckcenter Institute) for reviewing the manuscript, and Ms. Ayako Nakamura, Ms. Yasuko Kishimoto (Tokyo Metropolitan Institute for Neuroscience), and Ms. Yukiyo Numata (Tokyo Medical and Dental University) for technical assistance. This study was supported by Grant 22088 from Human Science, Japan.

1. Ben Hamida, C., Doerflinger, N., Belal, S., Linder, C., Reutenauer, L., Dib, C., Gyapay, G., Vignal, A., Le Paslier, D. & Cohen, D. (1993) *Nat. Genet.* **5,** 195–200.
2. Arita, M., Sato, Y., Miyata, A., Tanabe, T., Takahashi, E., Kayden, H. J., Arai, H. & Inoue, K. (1995) *Biochem. J.* **306,** 437–443.
3. Ouahchi, K., Arita, M., Kayden, H., Hentati, F., Ben Hamida, M., Sokol, R., Arai, H., Inoue, K., Mandel, J. L. & Koenig, M. (1995) *Nat. Genet.* **9,** 141–145.
4. Gotoda, T., Arita, M., Arai, H., Inoue, K., Yokota, T., Fukuo, Y., Yazaki, Y. & Yamada, N. (1995) *N. Engl. J. Med.* **333,** 1313–1318.
5. Yokota, T., Shiojiri, T., Gotoda, T. & Arai, H. (1996) *N. Engl. J. Med.* **335,** 1770–1771.
6. Yokota, T., Shiojiri, T., Gotoda, T., Arita, M., Arai, H., Ohga, T., Kanda, T., Suzuki, J., Imai, T., Matsumoto, H., Harino, S., Kiyosawa, M., Mizusawa, H. & Inoue, K. (1997) *Ann. Neurol.* **41,** 826–832.
7. Hosomi, A., Goto, K., Kondo, H., Iwatsubo, T., Yokota, T., Ogawa, M., Arita, M., Arai, H. & Inoue, K. (1998) *Neurosci. Lett.* **256,** 159–162.
8. Coyle, J. T. & Puttfarken, P. (1993) *Science* **262,** 689–695.
9. Cassarino, D. S. & Bettenn, J. P., Jr. (1999) *Brain Res. Rev.* **29,** 1–25.
10. Corasaniti, M. T., Strongoli, M. C., Rotiroti, D., Bagetta, G. & Nistico, G. (1998) *Pharmacol. Toxicol. (Copenhagen)* **83,** 1–7.
11. Burns, R. S., Chiueh, C. C., Markey, S. P., Ebert, M. H., Jacobowitz, D. M. & Kopin, I. J. (1983) *Proc. Natl. Acad. Sci. USA* **80,** 4546–4550.
12. Melov, S., Schneider, J. A., Day, B. J., Hinerfield, D., Coskun, P., Mirra, S. S., Crap, J. D. & Wallace, D. C. (1998) *Nat. Genet.* **18,** 159–163.
13. Jishage, K., Arita, M., Igarashi, K., Iwata, T., Watanabe, M., Ogawa, M., Ueda, O., Kamada, N., Inoue, K., Arai, H. & Suzuki, H. (2001) *J. Biol. Chem.* **276,** 1669–1672.
14. Abe, K. & Matsumoto, A. (1993) in *Vitamin E: Its Usefulness in Health and Curing Diseases*, eds. Mino, M., Nakamura, H. H. & Diplock, A. T. (Japan Scientific Societies, Tokyo), pp. 13–19.
15. Tamaoka, A., Miyatake, F., Matsuno, S., Ishii, K., Nagase, S., Sahara, N., Ono, S., Mori, H., Wakabayashi, K., Tsuji, S., Takahashi, H. & Shoji, S. (2000) *Neurology* **54,** 2319–2321.
16. Larnaout, A., Belal, S., Zouari, M., Fki, M., Ben Hamida, C., Goebel, H. H., Ben Hamida, M. & Hentati F. (1997) *Acta Neuropathol.* **93,** 633–637.
17. Yokota, T., Uchihara, T., Kumagai, J., Shiojiri, T., Pang, J. J., Arita, M., Arai, H., Hayashi, M., Kiyosawa, M., Okeda, R. & Mizusawa, H. (2000) *J. Neurol. Neurosurg. Psychiatry* **68,** 521–525.
18. Terasawa, Y., Ladha, Z., Leonardm, S. W., Morrow, J. D., Newland, D., Sanan, D., Packer, L., Traber, M. G. & Farese, R.V., Jr. (2000) *Proc. Natl. Acad. USA* **97,**13830–13834. (First Published November 28, 2000; 10.1073/pnas.240462697)
19. Simpson, E. M., Linder, C. C., Sargent, E. E., Davisson, M. T., Mobraaten, L. E. & Sharp, J. J. (1997) *Nat. Genet.* **16,** 19–27.
20. Hoshino, H., Masuda, N., Ito, Y., Mutara, M., Goto, J., Sakurai, M. & Kanazawa, I. (1999) *Ann. Neurol.* **45,** 809–812.
21. Gurney, M. E., Cutting, F. G., Zhai, P., Doble, A., Taylor, C. P., Andrus, P. K. & Hall, E. D. (1996) *Ann. Neurol.* **39,** 147–157.
22. Younkin, S. G. (2001) *Nat. Med* **7,** 18–19.
23. Yokota, T., Furukawa, T., Tsukagoshi, H., Mitakawa, H., Hasumura, Y. & Tsuchiya, K. (1990) *J. Neurol.* **237,** 103–106.
24. Esterbauer, H., Cheeseman, K. H., Dianzani, M. U., Poli, G. & Slater, T. F. (1982) *Biochem. J.* **208,** 129–140.
25. Esterbauer, H., Schaur, R. J. & Zollner, H. (1991) *Free Radical Biol. Med.* **11,** 81–128.
26. Malchet, V. G., Tappel, A. L. & Burns, M. (1974) *Lipids* **9,** 328–332.